



J. Serb. Chem. Soc. 91 (0) 1–17 (2026)
JSCS–13407

Adsorption of copper ions onto acid-modified *Aframomum africanum* shell: Isotherm and kinetic studies

YANE CHIMBILIMA, MURALI DADI and TANWEER AHMAD*

Department of Chemistry, School of Mathematics and Natural Sciences, The Copperbelt University, P.O. Box 21692, Kitwe, Zambia

(Received 3 June, revised 29 July 2025, accepted 23 February 2026)

Abstract: In this work, copper ions were successfully removed from aqueous solution using the acid-modified *Aframomum africanum* shell (MAAS) as an adsorbent. The adsorbent was characterized using Fourier transform infrared (FTIR) spectroscopy and field emission scanning electron microscopy (FESEM). The *A. africanum* shells were also characterized before and after acid modification to determine their pH at the point of zero charge (pH_{PZC}). MAAS was found to have a pH_{PZC} value of 4.77. In batch experiments, the adsorption capacity of MAAS was investigated as a function of solution pH, adsorbent dosage, contact time, initial copper ion concentration and agitation speed. The results revealed that at a solution pH of 9, an adsorbent dosage of 5 g/L, a contact time of 30 min, an initial Cu(II) ion concentration of 50 mg/L and at an agitation speed of 250 rpm, the maximum Cu(II) ion adsorption capacity of MAAS was 31.25 mg/g. The adsorption kinetic data and isotherm data were also studied to find the suitable models of Cu(II) removal. The kinetic data and the isotherm data of Cu(II) removal by MAAS were found to follow the pseudo-second order kinetics model ($R^2 = 0.999$) and the Langmuir isotherm model ($R^2 = 0.990$), respectively. Therefore, the outcome suggested that *A. africanum* shells can be utilized as an economical and efficient adsorbent for the removal of Cu(II) from aqueous solution.

Keywords: adsorption; *Aframomum africanum*; copper ion; heavy metal; adsorption kinetics; adsorption isotherms.

INTRODUCTION

The existence of life on this planet depends on the availability of water. Water is increasingly being contaminated anthropogenically by activities such as industrial activities, agriculture, poor land usage, urbanization and non-sustainable growth. These factors have led to rapid degradation of surface and groundwater quality.¹ Among these activities, the release of effluents containing heavy metals remains a

* Corresponding author. E-mail: tanweerakhan@gmail.com
<https://doi.org/10.2298/JSC250603010C>

serious concern, especially for humans and aquatic life in mining areas of the world. According to the Environmental Protection Agency (EPA), a heavy metal is one that has a higher density and potential toxicity even at a lower concentration.² By specifying the lower limit value of heavy metals, defines heavy metals as metals having density greater than 5 g/cm³.³ A common heavy metal, copper is employed in innovative applications, including solar cells and phytotherapies, as well as in decorative work and electric cable manufacturing. The element is an essential micronutrient for various processes such as photosynthesis, metabolism and reproduction processes in living organisms.⁴ However, high concentrations of non-biodegradable heavy metals, such as copper, in water bodies and in the soil have toxic effects on living organisms including humans.⁵ If humans are exposed to large doses of copper, degeneration or possibly necrosis of the kidneys, liver and gastrointestinal tract would be the outcome. Copper has also been linked to changes in the nervous system or mental health issues, including anxiety and insomnia.⁶

The physicochemical techniques have mostly been employed in heavy metal eradication processes such as chemical precipitation, membrane-based techniques, ion exchange and electrochemical processes.⁷ However, these remediation techniques have some drawbacks, such as high operational costs for metal complexes in trace concentrations, and high energy prerequisite.^{8,9} Efforts have been made to resolve these drawbacks by adopting the adsorption technique. The process of adsorption involves the migration and accumulation of dissolved molecules onto the surface and porous structure of a biomaterial. As adsorbents, activated carbons have been widely employed to remove harmful metal ions from wastewater. But owing to their high cost of production and regeneration challenges, there is now more effort being made to find adsorbent materials of low energy requirements, simplicity in operation and, of course, which can be regenerated.¹⁰ Examples of biomaterials that have been used before as adsorbents to eliminate heavy metals from wastewater include agricultural waste residues like groundnut shells, corn cob, rice husk and many more.¹¹ Adsorption has been found to exhibit the following advantages: cost-effectiveness, high efficiency, easy accessibility, minimal production of sludge, high adsorption capacity,¹² regeneration of adsorbents and possibility of metal recovery.¹³ Furthermore, the use of unconventional materials is being widely encouraged now owing to the fact that they possess functional groups that may bind metals.^{14–16}

The shell of the *Aframomum africanum* plant is another agricultural waste that may be a very good adsorbent for metal removal. Among a diverse range of affordable adsorbents, the *A. africanum* fruit shells (AAFS) were used as one of the promising, renewable, cost-effective biosorbents to eliminate Cu(II) ion from wastewater. *A. africanum* is a perennial, bushy and wild-growing plant with a leafy stem that may be up to 1.5 m high. The leaves are simple, alternate and lanceolate with matured ones measuring as long as 40 cm in length and 12–15 cm wide. The

plant is native to tropical African countries such as Ghana, Nigeria, Liberia and Cameroon and is an important commercial crop in east African countries such as Ethiopia. *A. africanum* fruit belongs to the family of *Zingiberaceae*.¹⁷ It is one of the highly consumed fruits in Zambia, which creates a notable environmental problem because the shells are usually thrown anyhow after the inner contents of the fruit have been eaten.¹⁸

To the best of the authors' knowledge, no studies have been done regarding the application of acid-modified *A. africanum* shell (MAAS) as an adsorbent for Cu(II) ion removal from aqueous solution. Therefore, this study was planned to assess the adsorption properties of the acid-modified *A. africanum* shell towards the removal of Cu(II) ions from aqueous solution. The surface functional groups and the morphology of the acid-modified *A. africanum* shells were evaluated before and after adsorption procedures. The experimental variables have been examined in relation to the removal of Cu (II), including the solution pH, initial metal concentration, particle size and contact time. Analysis of the experimental data has been done using kinetic and equilibrium isotherm models.

EXPERIMENTAL

Materials

Analytical grade chemicals were used. Copper (II) sulfate pentahydrate ($\text{CuSO}_4 \cdot 5\text{H}_2\text{O}$) was prepared by dissolving in distilled water for the experiment. The solution pH was adjusted from 2 to 12 using 0.1 M sodium hydroxide (NaOH) and 0.1 M hydrochloric acid (HCl). 0.5 M nitric acid (70 %, HNO_3) was utilized for the chemical treatment of the adsorbent.

Preparation of the adsorbent

The adsorbent *Aframomum africanum* fruit shell (AAFS) was procured from Chisokone market in Kitwe town of Zambia. The authenticity of the fruit was confirmed by the Department of Forest Herbarium Section under the Ministry of Green Economy in Kitwe Town. The fruit shell was washed thoroughly to remove dust and impurities using tap water. Later, the shells were sun-dried for 10 days and then oven-dried for 24 h at 80 °C to remove moisture from the shells properly. Dried shells were crushed in a blender and sieved by allowing the particles to pass through the 212- μm sieve. The powder obtained was again boiled in distilled water for 24 h to completely eliminate any coloration from the sample. Finally, the sample was dried in the oven for 24 h at 80 °C to remove moisture and stored in an air-tight bottle.

Chemical modification of the AAFS dried powder

The AAFS dried powder (82.58 g) was added to a 2 L conical flask that contained 0.5 M dilute nitric acid. The mixture was shaken for 2 h on an orbital shaker at 140 rpm and was left to stand for 24 h. After repeatedly washing the modified sample in distilled water to get rid of any remaining nitric acid, it was dried in an oven set at 60 °C for 48 h. The modified AAFS powder (now called MAAS) was stored in an air-tight bottle for later use. The flow diagram of *A. africanum* fruit shell drying and its conversion into acid-modified adsorbent is shown in Fig. 1.

Preparation of copper sulphate solution

To prepare a 1000 ppm Cu (II) sulphate stock solution, 3.93 g of copper (II) sulphate pentahydrate was dissolved in 1 L of distilled water. All subsequent Cu(II) ion concentration

solutions in this experiment were prepared by withdrawing the calculated volume of stock solution and diluting it in a volumetric flask of the required volume using distilled water only. To prepare a solution of a specific concentration, the dilution formula was used.

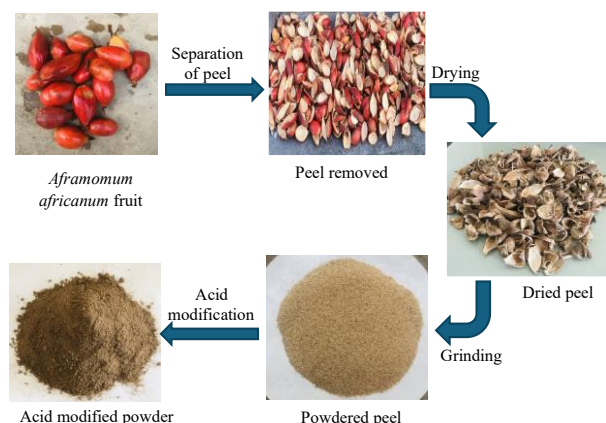


Fig. 1. Schematic representation of *Aframomum africanum* fruit shell drying and its conversion into acid-modified adsorbent.

Characterization of the adsorbent

The different functional groups on the adsorbent's surface were identified using Fourier transform infrared spectroscopy (FTIR, Alpha-II, Bruker, Germany). With a resolution range of 2–4 cm^{-1} , the FTIR spectra were captured before and after the Cu(II) adsorption within the wavenumber 400–4000 cm^{-1} region. The FESEM (JEOL-JST-IT80, Japan) was used to investigate the surface morphology of the adsorbent before and after the adsorption process.

The pH_{PZC} parameter was determined by placing 40 ml of an aliquot of sodium nitrate into 10 different Erlenmeyer flasks. The pH of the sodium nitrate solutions in the Erlenmeyer flasks was changed from 3 to 12 by reading values on the pH meter using 0.1 M HCl and 0.1 M NaOH solutions. To each flask, 5 g of the adsorbent was added and the flasks were shaken for 24 h. After equilibrium, the content was filtered, the final pH of the filtrate of each flask was measured and recorded. Finally, plots of change in pH (ΔpH , *i.e.*, initial pH – final pH) against initial pH (pH_i) were constructed.

Batch adsorption studies

In the batch experiment, 250 mL conical flasks were used to pour 100 mL of Cu(II) solution with the calculated amount of MAAS adsorbent. To get the concentration needed for each experiment, the Cu(II) solution was diluted with distilled water in a standard flask. The content of the conical flask was then agitated at a fixed number of revolutions per minute on a shaker, for a fixed contact time and at room temperature. After that, filter paper was used to separate the adsorbent from the mixture. The residual concentrations of Cu ions were measured using an atomic absorption spectrophotometer (contraAA 300, Analytik Jena, Germany.)

The adsorption capacity (amount of adsorption) of the adsorbent at equilibrium, q_e (mg/g), and the percentage of heavy metal removal R (%) were determined as:

$$q_e = \frac{c_i - c_e}{m} V \quad (1)$$

$$R = 100 \frac{c_i - c_e}{c_i} \quad (2)$$

where m is the dry weight of the adsorbent (g), V is the volume of the Cu(II) ions in solution (L), c_i is the initial Cu(II) ion concentration (mg/L) and c_e is the Cu(II) ion concentration (mg/L) at equilibrium.

The effect of independent variables, such as contact time (5–120 min), and initial Cu(II) concentration (10–150 mg/L) on the adsorption capacity of MAAS adsorbent against Cu(II) was observed at a fixed temperature (25 °C), fixed volume of Cu(II) solution (100 mL) and adsorbent dosage (5.0 g/L). The effect of varying each individual parameter was investigated while holding the other parameters constant. To calculate the kinetic parameters, the adsorption data of Cu(II) against time were used and to calculate the isotherm parameters, the adsorption data of Cu(II) against its equilibrium concentration was equally exploited. Additionally, regression coefficients (R^2) were calculated for the adsorption kinetics and the isotherms.

RESULTS AND DISCUSSION

FTIR analysis of the MAAS

It is crucial to identify the chemical functional groups on the adsorbent's surface in order to understand the adsorption mechanism of Cu(II) by the adsorbent. The chemical functional groups present could be responsible for the metal ion binding onto the surface of the adsorbent.¹⁹ As seen in Fig. 2, the FTIR spectrum of MAAS before adsorption contains hydroxyl groups (–O–H) and phenols as well as the –N–H group indicated by the broad transmission peak at 3365.²⁰ The asymmetric C–H stretching of surface methyl groups, which are often found in the lignin structure, is indicated by the peak at 2917 cm^{-1} .^{21,22} The band observed around 1637 cm^{-1} is due to the C=O stretching of the carbonyl group. The C–O stretching of alcohol and carboxylic acid groups in cellulose, hemicelluloses and lignin or C–O–C stretching in cellulose and hemicellulose, was identified by the strong band at 1043 cm^{-1} .²⁰ The role played by these functional groups is quite important in heavy metal adsorption because of the functional groups' affinity for metal ions.

The FTIR spectrum of post adsorption MAAS (MAAS–Cu) is shown in Fig. 2 as well. It was observed that the post adsorption spectra had peaks at exactly the same wavenumber as the pre-adsorption spectra. However, a reduction in peak intensities was observed. The reduction in peak intensities suggests the involvement of various functional groups in complexation with Cu(II) without undergoing major chemical transformation. Additionally, this showed that the copper adsorption mechanism involved a large number of functional groups found in the spectra.⁹

FESEM analysis of MAAS

Using FESEM, the surface morphology of MAAS was analyzed before and after the adsorption of Cu(II) ions. Fig. 3a shows the surface morphology of the

adsorbent before Cu(II) adsorption, while Fig. 3b represents Cu(II) adsorbed onto the surface of MAAS.

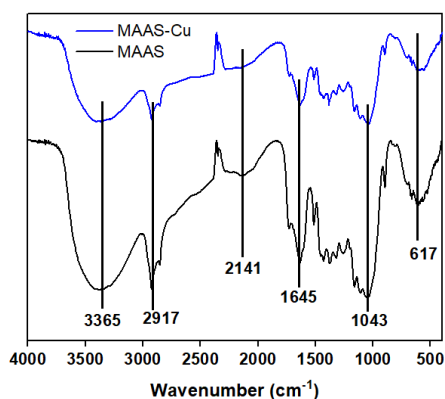


Fig. 2. FTIR spectra for the acid-treated adsorbent.

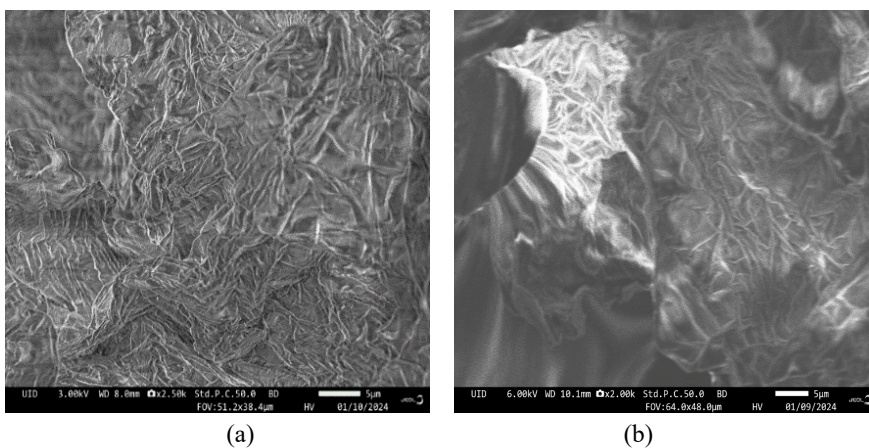


Fig. 3. FESEM images of MAAS before (a) and after (b) adsorption of Cu(II).

Pre-adsorption surface of MAAS (Fig. 3a) contains pores and cavities on a rough and uneven surface of the acid-modified adsorbent. The post-adsorption MAAS surface pores were covered with Cu(II) ions, as seen in Fig. 3b, and the majority of the pores became invisible. Furthermore, the post-adsorption MAAS surface became somewhat smoother. This indicated that the surface pores were covered with Cu(II) ions.

Point of zero charge

It is the pH at which the adsorbent surface has no net charge. The pH_{PZC} of MAAS was determined for both the untreated adsorbent and the nitric acid-treated adsorbent. The results are shown in Fig. 4. The acid-modified adsorbent had a

pH_{PZC} of 4.77, which means that at pH values lower than this its surface is positively charged and at pH higher than 4.77 the adsorbent's surface is negatively charged. The pH_{PZC} of the untreated adsorbent was 7.62.

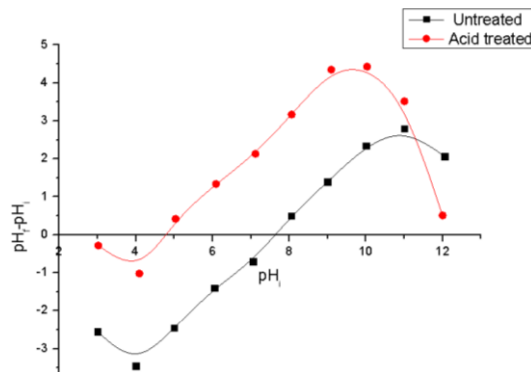


Fig. 4. pH_{PZC} of the untreated and treated adsorbent.

Effect of solution pH

The most significant parameter affecting the adsorption of Cu(II) ions onto MAAS is the solution pH. It establishes the adsorbent's surface charge as well as the adsorbate's degree of ionization and speciation.²³ The pH of the Cu(II) solutions was changed from 2 to 12 while maintaining the same initial concentration of 50 mg/L, contact time of 60 min, agitation speed of 150 rpm, and dosage of 5 g/L. From the experiment, maximum adsorption was 99.73 % at pH 9. The percentage of copper removed was low at low pH. The adsorbent surface is positively charged if the pH of the solution is lower than the pH_{PZC} . Conversely, for a solution pH greater than pH_{PZC} , deprotonation causes the adsorbent surface to become negatively charged, which promotes Cu(II) and the adsorbent surface's electrostatic attraction and raises the adsorption percentage.⁹ This is explained by the extra H^+ that surrounds the binding sites and causes a protonation process that makes them positively charged. This results in the repulsion of metal cations away from the adsorption sites, making the adsorption process unfavorable. Additionally, the presence of H^+ in solution results in competitive adsorption between the H^+ and metal cations. This leads to competition between H^+ and Cu(II) for the adsorbent's adsorption sites, which results in repulsion.^{24,25} Thus, pH 9 was chosen for the subsequent adsorption studies because it is above the pH_{PZC} . Above pH 9 the percentage removal of Cu(II) decreased. This may be due to the hindrance effect caused by the abundant OH^- (hydroxide precipitation) preventing the diffusion of Cu(II) onto the adsorbent. The results are shown in Fig. 5a.

Effect of adsorbent dose

To explore the influence of adsorbent dosage on the elimination of copper from wastewater, the dosage was varied from 0.5, 1.0, 2.0, 3.0, 4.0 and 5.0 g/L

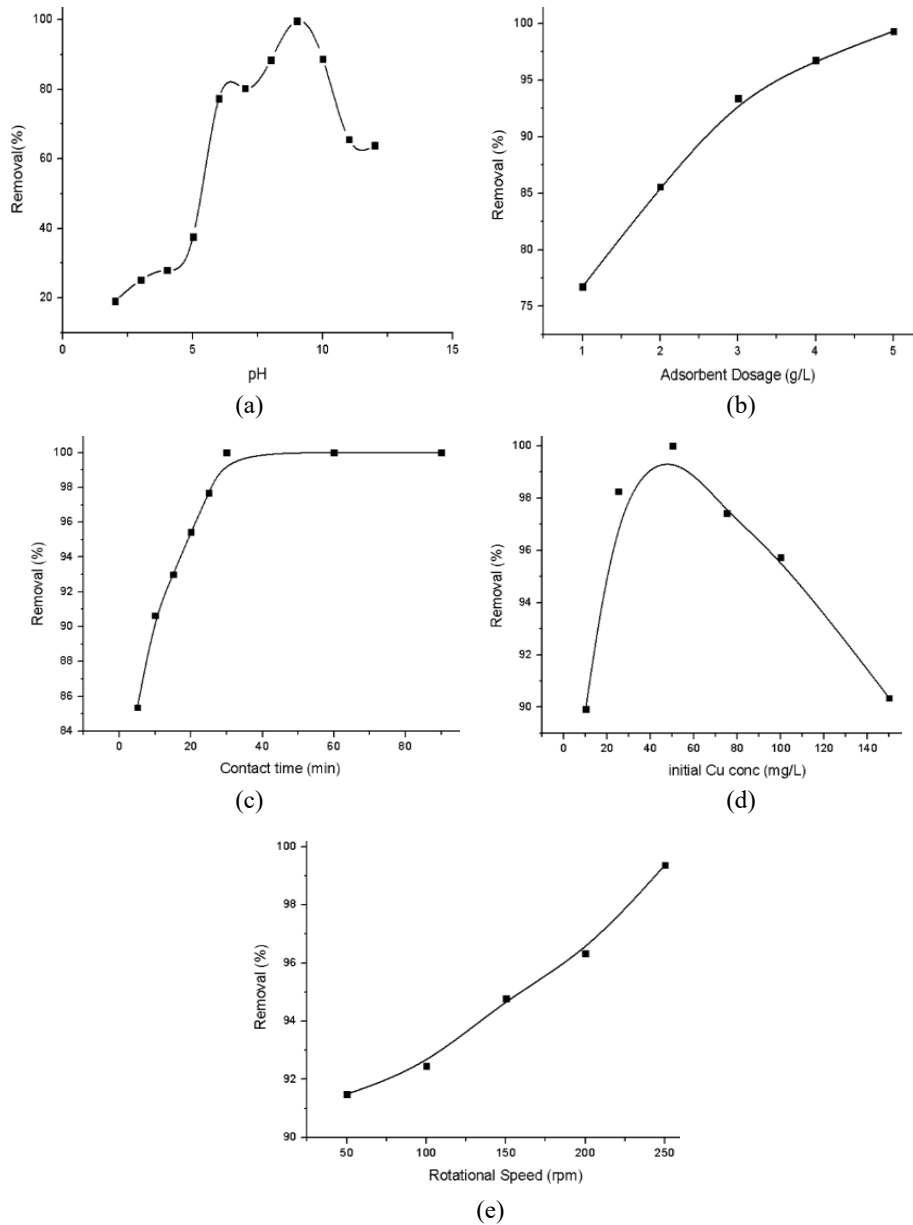


Fig. 5. Effect of: a) solution pH, b) adsorbent dosage, c) contact time, d) initial Cu(II) concentration and e) rotational speed on Cu ion removal efficiency.

while keeping other parameters unchanged (pH 9, contact time 60 min, initial concentration 50 mg/L and agitation speed 150 rpm). The results in Fig. 5b show that the removal efficiency increased with increasing adsorbent dosage, producing

the highest efficiency removal of 99.33 % at a dosage of 5 g/L. The increased percentage removal can be attributed to the number of available adsorption sites, which increased with the mass of the adsorbent.²⁶ Therefore, an optimal adsorbent dosage of 5 g/L was used in the follow-up adsorption experiments.

Effect of contact time

The time of contact between the adsorbent and the aqueous metal solution is another parameter which influences the uptake of metal ions. At constant parameters (pH 9, adsorbent dose 5 g/L, initial concentration 50 mg/L and agitation speed 150 rpm), studying the effect of contact time (5, 10, 20, 30, 60, 90 and 120 min) on the removal percentage of Cu(II), the results are revealed in Fig. 5c. From the graph, the greatest removal efficiency of Cu(II) was more pronounced during the first 30 min. This is attributed to the availability of vacant sorption sites of the adsorbent during the initial stage of the adsorption process.²⁷ After 30 min, the amount of Cu(II) adsorbed remained unchanged. This could be due to the active sites present on the adsorbent's surface being saturated by the Cu (II) molecules.

Effect of initial Cu(II) concentration

The effect of initial Cu(II) concentration on the removal efficiency was investigated for different solution concentrations of 10, 25, 50, 75, 100 and 150 mg/L while ensuring that the other parameters were kept constant. From the experimental results, the percentage removal of Cu(II) increased with the increase of Cu(II) concentration from 10 to 50 mg/L. As can be seen from Fig. 5d, the removal efficiency increased from 89.93 % for the initial Cu(II) concentration of 10 mg/L to 100 % for the initial Cu(II) concentration of 50 mg/L after the adsorption process. However, from 50 mg/L, further increase in the initial Cu(II) concentration resulted in a decreased removal efficiency. This reduced removal at higher initial concentrations is attributed to the adsorbent's surface being saturated at the relatively high metal concentration¹³ and also desorption may have occurred.²⁸

Effect of agitation speed

The influence of varying the speed of agitation at 50, 100, 150, 200 and 250 rpm was also investigated while maintaining other parameters constant (pH 9, adsorbent dose 5g/L, 30 min of contact time and initial metal concentration 50 mg/L). From the experimental results obtained in Fig. 5e, the removal efficiency increased with an increase in the speed of agitation. The results show a maximum removal percentage of almost 100 % at an agitation speed of 250 rpm. At low speeds, the adsorbent accumulates at the bottom instead of spreading throughout the solution. The result is that the sorption sites below the above layers of the adsorbent get buried leading to the low removal percentage of the metal ions.

Therefore, the speed of agitation of the adsorbate-adsorbent mixture should be sufficient enough to ensure the adsorbent spreads throughout the solution so that the unoccupied binding sites are exposed for the metal uptake.²⁹

Adsorption isotherm studies

In order to investigate the distribution of Cu(II) ions between the adsorbent and the bulk solution, the most common adsorption isotherm models were used by fitting the equilibrium adsorption data into their respective isotherm equations.³⁰ The adsorption isotherm models used were the Langmuir, Freundlich, Temkin and Dubinin–Radushkevich (D–R) isotherm models.

Langmuir adsorption isotherm. The Langmuir adsorption isotherm model suggests that the adsorption of adsorbate molecules onto the adsorbent surface is a monolayer³¹ and that the adsorbent has a finite number of homogeneously distributed and energetically uniform sorption sites. Therefore, this model applies to adsorption on adsorbent surfaces which are entirely homogeneous. A plot of c_e/q_e vs. c_e should yield a straight line if the Langmuir isotherm model is obeyed by the adsorption equilibrium as shown in Fig. 6a. From the plot, q_m and K_L values can be evaluated, which are obtained from the slope ($1/q_m$) and the intercept ($1/q_m K_L$), respectively.

An important aspect of the Langmuir isotherm called the separation factor, R_L (a dimensionless constant), is very useful in predicting the affinity between the adsorbate and the adsorbent.³² The separation factor, which is also called the equilibrium parameter, is defined as:

$$R_L = \frac{1}{1 + K_L c_i} \quad (3)$$

By determining the magnitude of the separation factor, the adsorption process is favorable within the range $0 < R_L < 1$, unfavorable when $R_L > 1$, linear when $R_L = 1$, and the process is irreversible when $R_L = 0$. The Langmuir constant ($K_L = 0.508$ L/mg) indicates a strong affinity between the adsorbent and the adsorbate. Furthermore, the separation factor ($R_L = 0.04$), being closer to zero, confirms highly favorable adsorption. Table I shows that adsorption follows the Langmuir isotherm model ($R^2 = 0.99$) with a q_{\max} value of 31.25 mg/g. Modified *A. africanum* shell has a higher biosorption capacity for Cu(II) ion removal than most of the biosorbents previously described in the literature.^{33–36}

Freundlich adsorption isotherm. The Freundlich adsorption isotherm suggests that the uptake of adsorbate solutes occurs on the heterogeneous surface of an adsorbent by multilayer adsorption. The model's assumption is that the uptake of sorbate molecules occurs on the heterogeneous surface of an adsorbent by multilayer adsorption.³⁷ This isotherm model describes adsorbents whose active sites have different affinities or adsorption energies for adsorbate solutes. The values of the

Freundlich constants can be obtained by plotting $\ln q_e$ vs. $\ln c_e$ with $\log k_F$ as the intercept and the slope equal to $1/n$ shown in Fig. 6b. The magnitude of n indicates the favorability of biosorption. If the value of $n < 1$ then the biosorption is unfavorable, when $n = 1$ then the separation within the two phases is not dependent on the concentration and when $n > 1$, it implies the adsorption of the adsorbate molecules onto the adsorbent surface is favorable. The Freundlich constant ($k_F = 9.92 \text{ mg}^{1-1/n} \text{ L}^{1/n} \text{ g}^{-1}$) indicates a high adsorption capacity of the adsorbent. The value of $1/n = 0.412$ ($n = 2.43$) suggests favorable adsorption on a heterogeneous surface. However, the comparatively lower R^2 value indicates that the Freundlich isotherm provides a weaker fit than the Langmuir isotherm. The values of n and k_F calculated using slope and intercept were 2.42 and 9.92 with $R^2 = 0.862$ as shown in Table I. Consequently, adsorption has been conducted as a chemical process since the value of $n > 1$.

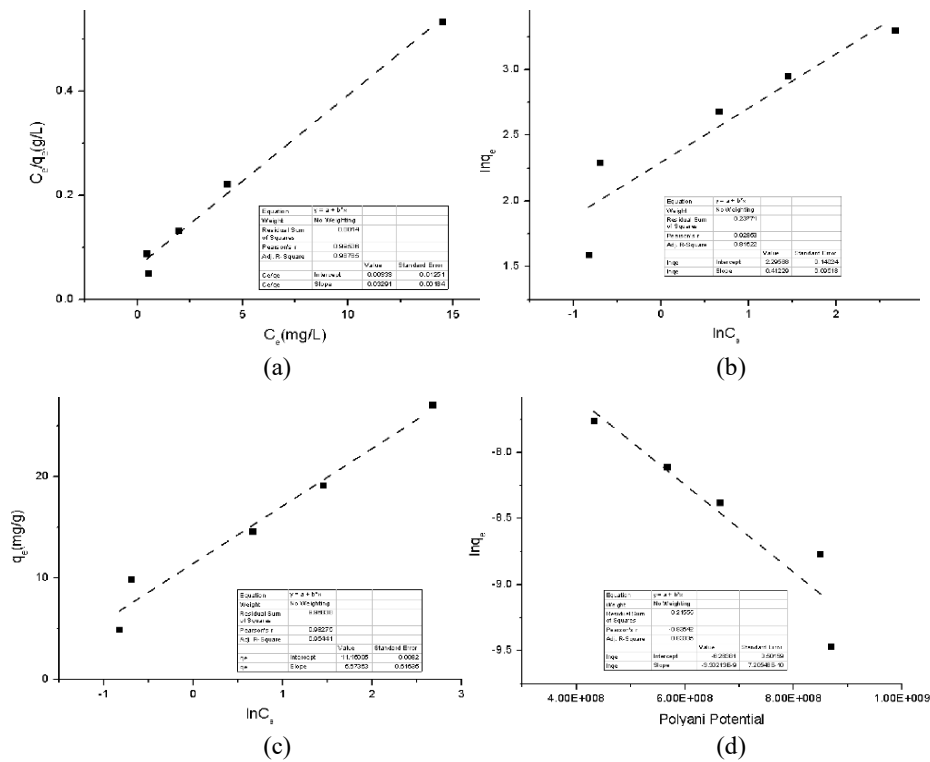


Fig. 6. Adsorption isotherm plots of Cu(II) removal through MAAS; a) Langmuir linear model, b) Freundlich linear model plot, c) Temkin isotherm linear model plot and d) D-R isotherm linear model.

Temkin adsorption isotherm. The heat involved in the adsorption of Cu(II) on MAAS was evaluated through the Temkin isotherm. It is assumed that the decline

in the heat of adsorption followed a linear trend as opposed to a logarithmic curve.³⁸ As illustrated in Fig. 6c, the slope of the q_e vs. $\ln c_e$ plot can be used to compute the heat of adsorption constant (B). The Temkin constant B (436.73 J/mol) indicates a moderate heat of adsorption, suggesting that the process is predominantly physical in nature. The equilibrium binding constant ($K_T = 7.52$ L/mg) reflects a good affinity between the adsorbent and the adsorbate. Table I provides a summary of the computed values for the Temkin isotherm constants and associated parameters. The computed values are close to the actual heat involved in the adsorption, as indicated by the model's correlation coefficient for Cu(II) adsorption data, which was determined to be 0.985.

Dubinin–Radushkevich (D–R) adsorption isotherm. The D–R isotherm assumes that the sorption sites are not identical and takes into account the idea of adsorbent surface heterogeneity, just like the Freundlich isotherm does.³⁹ The D–R model's linearized form is provided as:

$$\ln q_e = \ln q_{\max} - \beta \varepsilon^2 \quad (4)$$

where ε ($\text{kJ}^2 \text{mol}^{-2}$) is the Polanyi potential and β (mol^2/J^2) is the activity coefficient associated with the mean adsorption energy.

The following relation was used to derive the Polanyi potential:⁴⁰

$$\varepsilon = RT \ln(1 + 1/c_e) \quad (5)$$

The mean free energy of adsorption (E_A) per molecule of adsorbate can be calculated using the D–R isotherm constant (K_{D-R}) when the adsorbate molecules migrate from infinity to the adsorbent surface. It can be computed as:

$$E_A = \frac{1}{\sqrt{2K_{D-R}}} \quad (6)$$

Table I lists the D–R isotherm constants for Cu(II) adsorption onto MAAS along with the associated mean free energy of adsorption. The type of the adsorbent and the adsorbate determine the adsorption potential, which is unaffected by temperature. It is possible to determine whether adsorption is physical or due to chemical ion exchange by examining the E_A . The adsorption phase that comes after the chemical ion exchange is shown by the values of E_A that fall between 8 and 16 kJ/mol. The average free energy for this adsorption ($E_A = 12.90$ kJ/mol) falls within the range, indicating that ion-exchange followed the adsorption mechanism. The D–R constant β ($3.00 \times 10^{-9} \text{ mol}^2/\text{J}^2$) suggests a narrow energy distribution and supports adsorption occurring predominantly in microporous region of the adsorbent. Fig. 5d displays the linearized D–R plot, and the linear plot's correlation coefficient (R^2) was determined to be 0.875. As a result, the Langmuir isotherm was better suited by the adsorption data than the Freundlich, Temkin and D–R isotherm models.

TABLE I. The parameter values of adsorption isotherm models of Cu(II) adsorption onto modified *Aframomum africanum* shells at 25 °C

Model	Model parameter	Value
Langmuir	$q_{\max} / \text{mg g}^{-1}$	31.25
	$K_L / \text{L mg}^{-1}$	0.508
	R_L	0.04
	R^2	0.99
Freundlich	$K_F / \text{mg}^{1-1/n} \text{L}^{1/n} \text{g}^{-1}$	9.92
	$1/n$	0.412
	R^2	0.862
Temkin	$B / \text{J mol}^{-1}$	436.73
	$K_T / \text{L mg}^{-1}$	7.52
	R^2	0.985
D-R	$q_{\max} / \text{mg g}^{-1}$	121.1
	$q_{\max} / \text{mmol g}^{-1}$	1.91
	$E_A / \text{kJ mol}^{-1}$	12.9
	β	3.00×10^{-9}
	R^2	0.875

Adsorption kinetic study

During adsorption studies, determining the rate and comprehending the mechanism of heavy metal adsorption are crucial. In order to fit the experimental results, various kinetic models have been presented.⁴¹ The pseudo-first-order kinetic model and the pseudo-second-order kinetic models are the only two kinetic models covered in this study.

Pseudo-first-order kinetics model (PFO). As illustrated in Fig. 7a, linear plots of $\log(q_e - q_t)$ versus t suggest the applicability of this kinetic model. From the graph, k_1 can be computed.

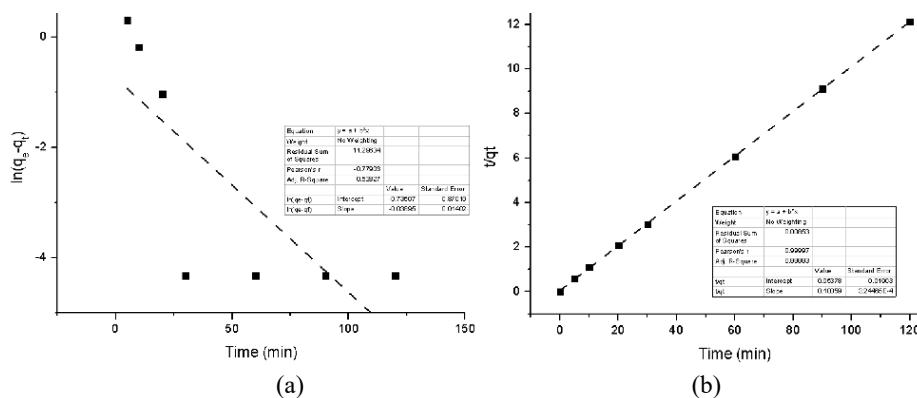


Fig. 7. Adsorption kinetics of Cu(II) removal: a) pseudo-first and b) pseudo-second order kinetic model plot.

Pseudo-second-order kinetics model (PSO). The mechanism of adsorption is assumed to follow a second-order kinetics model if a plot of t/q_t against t produces a straight-line graph. The plot's slope ($1/q_e$) and intercept ($1/k_2q_e^2$) yield the values of q_e and k_2 , respectively.

A well-established kinetic models, PFO and PSO were used to study the adsorption kinetics of Cu(II) adsorption onto MAAS. The Cu(II) adsorption data were collected at 50 mg/L an initial concentration at different time intervals (from 5 min to 120 min) and applied to linearized PSO shown in Fig. 7a and b. Within 30 min of contact time, 99 % of adsorption was found to occur. PFO and PSO were used to visualize the collected kinetic data. From the plotted data, it was observed that Cu(II) adsorption onto MAAS poorly followed the PSO ($R^2 = 0.606$) shown in Fig. 7a but perfectly followed the PSO kinetic model. The linear curve fitting of the PFO and PSO gave the correlation coefficient (R^2) value of 0.999 shown in Fig. 7b. It was also observed that for PSO kinetics, the theoretical adsorption capacity $q_{e,cal}$ (10.00 mg/g) and experimental values $q_{e,exp}$ (9.901 mg/g) were extremely close, however for PFO kinetics, these values were different, Table II. The PSO kinetics model was therefore more applicable, as evidenced by the same values for $q_{e,cal}$ and $q_{e,exp}$ and a higher regression coefficient value ($R^2 = 0.99$) compared to the PFO ($R^2 = 0.606$).

TABLE II. The parameter values of adsorption kinetic models of Cu(II) ion adsorption by modified *Aframomum africanum* shells

Model	Model parameter	Value
Pseudo-first-order	$q_e / \text{mg g}^{-1}$	0.478
	k_1 / min^{-1}	0.038
	R^2	0.606
Pseudo-second-order	$q_e / \text{mg g}^{-1}$	10
	$k_2 / \text{g mg}^{-1} \text{min}^{-1}$	0.189
	R^2	0.999

CONCLUSION

In the present study, low-cost adsorbents were successfully prepared from *Aframomum africanum* fruit through chemical surface modification. Nitric acid was used to modify the fruit shell powder, FESEM and FTIR were used to observe the changes in the adsorbent surface. The adsorption of Cu(II) from aqueous solution by the acid-modified adsorbent was investigated under various conditions of pH, adsorbent dosage, contact time, initial Cu(II) concentration and agitation speed. Among these conditions, pH was found to be the most significant factor affecting the adsorption of Cu(II). For a dosage of 5 g/L, a contact time of 30 min and an initial Cu(II) concentration of 50 mg/L, the maximum removal of Cu(II) was 100 % at pH 9. The Langmuir isotherm model and the pseudo-second-order kinetic model were able to adequately fit the experimental results. The Langmuir isotherm predicted monolayer

adsorption of Cu(II) ions with a maximum adsorption capacity of 31.25 mg/g. *A. africanum* is an effective adsorbent for the sequestration of Cu (II) from aqueous solution, according to the experimental data.

Acknowledgement. Thanks to Department of Chemistry, School of Mathematics and Natural Sciences, The Copperbelt University for laboratory facilities.

ИЗВОД

АДСОРПЦИЈА ЈОНА БАКРА НА КИСЕЛИНОМ МОДИФИКОВАНУ ЉУСКУ *Aframomum africanum*: ИЗОТЕРМСКА И КИНЕТИЧКА ИСПИТИВАЊА

YANE CHIMBILIMA, MURALI DADI и TANWEER AHMAD

Department of Chemistry, School of Mathematics and Natural Sciences, The Copperbelt University, P.O. Box 21692, Kitwe, Zambia

У овом раду јони бакра су успешно уклоњени из воденог раствора применом киселином модификоване љуске *Aframomum africanum* (MAAS) као адсорбента. Адсорбент је окарактерисан применом инфрацрвене спектроскопије са Фуријеовом трансформацијом (FTIR) и скенирајуће електронске микроскопије са емисијом поља (FESEM). Љуске *A. africanum* су такође окарактерисане пре и после киселинске модификације ради одређивања рН вредности на тачки нултог наелектрисања (рН_{рзс}). Утврђено је да MAAS има рН_{рзс} вредност од 4,77. У серији експеримената испитиван је адсорпциони капацитет MAAS у зависности од рН вредности раствора, дозе адсорбента, времена контакта, почетне концентрације јона бакра и брзине мешања. Резултати су показали да је при рН вредности раствора од 9, дози адсорбента од 5 g/L, времену контакта од 30 min, почетној концентрацији Cu(II) јона од 50 mg/L и брзини мешања од 250 rpm постигнут максимални адсорпциони капацитет MAAS за Cu(II) јоне од 31,25 mg/g. Кинетички подаци и подаци изотерме адсорпције анализирани су ради одређивања одговарајућих модела уклањања Cu(II). Утврђено је да кинетички подаци прате модел псеудо-другог реда ($R^2 = 0,999$), док изотермски подаци прате Ленгмиров модел изотерме ($R^2 = 0,990$). Резултати указују да се љуске *A. africanum* могу користити као економичан и ефикасан адсорбент за уклањање Cu(II) јона из водених раствора.

(Примљено 13. јуна, ревидирано 30. јуна, прихваћено 2. децембра 2026)

REFERENCES

1. A. Hussain, S. Madan, R. Madan, in *Heavy Metals - Their Environmental Impacts and Mitigation*, M. K. Nazal, H. Zhao, Eds., Intech Open, Rijeka, 2021 (<https://doi.org/10.5772/intechopen.95841>)
2. D. Piwowska, E. Kiedrzyńska, K. Jaszczyszyn, *Crit. Rev. Environ. Sci. Technol.* **54** (2024) 1436 (<https://doi.org/10.1080/10643389.2024.2317112>)
3. P. B. Angon, M. S. Islam, K. C. Shreejana, A. Das, N. Anjum, A. Poudel, S. A. Suchi, *Heliyon* **10** (2024) e28357 (<https://doi.org/10.1016/j.heliyon.2024.e28357>)
4. M. Rehman, L. Liu, Q. Wang, M. H. Saleem, S. Bashir, S. Ullah, D. Peng, *Environ. Sci. Pollut. Res.* **26** (2019) 18003 (<https://doi.org/10.1007/s11356-019-05073-6>)
5. S. Mitra, A. J. Chakraborty, A. M. Tareq, T. B. Emran, F. Nainu, A. Khuro, A. M. Idris, M. U. Khandaker, H. Osman, F. A. Alhumaydhi, J. Simal-Gandara, *J. King Saud Univer. – Sci.* **34** (2022) 101865 (<https://doi.org/10.1016/j.jksus.2022.101865>)

6. J. Briffa, E. Sinagra, R. Blundell, *Heliyon* **6** (2020) e04691 (<https://doi.org/10.1016/j.heliyon.2020.e04691>)
7. N. A. A. Qasem, R. H. Mohammed, D. U. Lawal, *npj Clean Water* **4** (2021) 36 (<https://doi.org/10.1038/s41545-021-00127-0>)
8. S. Maiti, B. Prasad, A. K. Minocha, *SN Appl. Sci.* **2** (2020) 2151 (<https://doi.org/10.1007/s42452-020-03892-8>)
9. C. I. Orozco, M. S. Freire, D. Gómez-Díaz, J. González-Álvarez, *Sustain. Chem. Pharm.* **32** (2023) 101016 (<https://doi.org/10.1016/j.scp.2023.101016>)
10. T. Ahmad, M. Danish, M. Dadi, K. Siraj, T. Sundaram, D. S. Raj, S. Majeed, S. Ramasamy, *J. Water Process Eng.* **67** (2024) 106113 (<https://doi.org/10.1016/j.jwpe.2024.106113>)
11. A. M. Elgarahy, K. Z. Elwakeel, S. H. Mohammad, G. A. Elshoubaky, *Cleaner Eng. Technol.* **4** (2021) 100209 (<https://doi.org/10.1016/j.clet.2021.100209>)
12. A. Nurain, P. Sarker, M. S. Rahaman, M. M. Rahman, M. K. Uddin, *J. Multidisc. Appl. Nat. Sci.* **1**(2021) 117 (<https://doi.org/10.47352/jmans.v1i2.89>)
13. A. Karnwal, *Desal. Water Treat.* **319**(2024) 100523 (<https://doi.org/10.1016/j.dwt.2024.100523>)
14. U. M. Ismail, M. S. Vohra, S. A. Onaizi, *Environ. Res.* **251** (2024) 118562 (<https://doi.org/10.1016/j.envres.2024.118562>)
15. C. Duan, T. Ma, J. Wang, Y. Zhou, *J. Water Process Eng.* **37** (2020) 101339 (<https://doi.org/10.1016/j.jwpe.2020.101339>)
16. O. A. Ramírez Calderón, O. M. Abdeldayem, A. Pugazhendhi, E. R. Rene, *Curr. Pollut. Rep.* **6** (2020) 8 (<https://doi.org/10.1007/s40726-020-00135-7>)
17. E. Fischer, B. E. N. Kirunda, C. Ewango, M. Leal, D. Kujirakwinja, A. Bamba, A. J. Plumptre, *Phytotaxa* **298** (2017) 277 (<https://doi.org/10.11646/phytotaxa.298.3.7>)
18. R. H. M. Knippers, S. Gallois, T. van Andel, *Econ. Bot.* **75** (2021) 76 (<https://doi.org/10.1007/s12231-021-09517-4>)
19. M. Danish, R. Hashim, M. N. M. Ibrahim, M. Rafatullah, O. Sulaiman, T. Ahmad, M. Shamsuzzoha, A. Ahmad, *J. Chem. Eng. Data* **56** (2011) 3607 (<https://doi.org/10.1021/je200460n>)
20. A. Chand, P. Chand, G. G. Khatri, D. R. Paudel, *Chem. Biochem. Eng. Q.* **35** (2021) 279 (<https://doi.org/10.15255/CABEQ.2021.1943>)
21. S. O. Owalude, A. C. Tella, *Beni-Suef Univer. J. Basic Appl. Sci.* **5** (2016) 377 (<https://doi.org/10.1016/j.bjbas.2016.11.005>)
22. E. Šabanović, M. Memić, J. Sulejmanović, A. Selović, *Polish J. Chem. Technol.* **22** (2020) 46 (<https://doi.org/10.2478/pjct-2020-0007>)
23. N. K. Berber-Villamar, A. R. Netzahuatl-Muñoz, L. Morales-Barrera, G. M. Chávez-Camarillo, C. M. Flores-Ortiz, E. Cristiani-Urbina, *PLoS One* **13** (2018) e0196428 (<https://doi.org/10.1371/journal.pone.0196428>)
24. Y. Liu, H. Wang, Y. Cui, N. Chen, *Int. J. Environ. Res. Pub. Health* **20** (2023) 3885 (<https://doi.org/10.3390/ijerph20053885>)
25. J. Aravind, S. Muthusamy, S. H. Sunderraj, L. Chandran, K. Palanisamy, *Int. J. Ind. Chem.* **4** (2013) 25 (<https://doi.org/10.1186/2228-5547-4-25>)
26. M. M. John, A. Benettayeb, M. Belkacem, C. Ruvimbo Mitchel, M. Hadj Brahim, I. Benettayeb, B. Haddou, S. Al-Farraj, A. A. Alkahtane, S. Ghosh, C. H. Chia, M.

- Sillanpaa, O. Baigenzhenov, A. Hosseini-Bandegharai, *Chemosphere* **357** (2024) 142051 (<https://doi.org/10.1016/j.chemosphere.2024.142051>)
27. A. A. Alghamdi, A.-B. Al-Odayni, W. S. Saeed, A. Al-Kahtani, F. A. Alharthi, T. Aouak, *Materials* **12** (2019) 2020 (<https://doi.org/10.3390/ma12122020>)
 28. H. Urooj, T. Javed, M. B. Taj, M. N. Haider, *Int. J. Environ. Anal. Chem.* **104** (2023) 7474 (<https://doi.org/10.1080/03067319.2023.2176229>)
 29. S. Dey, G. T. N. Veerendra, A. V. Phani Manoj, S. S. A. Babu Padavala, *Waste Manage. Bulletin* **2** (2024) 76 (<https://doi.org/10.1016/j.wmb.2024.09.006>)
 30. S. U. Khan, F. U. Khan, I. U. Khan, N. Muhammad, S. Badshah, A. Khan, A. Ullah, A. S. Khan, H. Bilal, A. Nasrullah, *Desalin. Water Treat.* **57** (2016) 3964 (<https://doi.org/10.1080/19443994.2014.989268>)
 31. I. Langmuir, *J. Am. Chem. Soc.* **38** (1916) 2221 (<https://doi.org/10.1021/ja02268a002>)
 32. K. Y. Foo, B. H. Hameed, *Chem. Eng. J.* **156** (2010) 2 (<https://doi.org/10.1016/j.cej.2009.09.013>)
 33. G. Annadurai, R.-S. Juang, D. Lee, *Water Sci. Technol.* **47** (2003) 185 (<https://doi.org/10.2166/wst.2003.0049>)
 34. B. Singha, S. K. Das, *Colloids Surfaces, B* **107** (2013) 97 (<https://doi.org/10.1016/j.colsurfb.2013.01.060>)
 35. M. A. Fawzy, H. M. Al-Yasi, T. M. Galal, R. Z. Hamza, T. G. Abdelkader, E. F. Ali, S. H. A. Hassan, *Sci. Rep.* **12** (2022) 8583 (<https://doi.org/10.1038/s41598-022-12233-1>)
 36. N. S. M. Tahiruddin, R. A. Aziz, R. Ali, N. I. Taib, *J. Environ. Chem. Eng.* **11** (2023) 109953 (<https://doi.org/10.1016/j.jece.2023.109953>)
 37. J. G. Amrutha, C. R. Girish, B. Prabhu, K. Mayer, *Environ. Process.* **10** (2023) 38 (<https://doi.org/10.1007/s40710-023-00631-0>)
 38. M. J. Temkin, V. Pyzhev, *Acta Physicochim. URSS* **12** (1940) 217
 39. M. M. Dubinin, E. D. Zaverina, L. V. Radushkevich, *Zh. Fiz. Khim.* **21** (1947) 1351
 40. M. Polanyi, *Trans. Faraday Soc.* **28** (1932) 316
 41. Z. Raji, A. Karim, A. Karam, S. Khalloufi, *Waste* **1** (2023) 775 (<https://doi.org/10.3390/waste1030046>).